The equilibrium crystal shape of strontium titanate and its relationship to the grain boundary plane distribution

Wolfgang Rheinheimer,[a,*] Michael Bäurer,[b] Harry Chien,[c] Gregory S. Rohrer,[d] Carol A. Handwerker,[e] John E. Blendell[e] and Michael J. Hoffmann[a]

[a]Institute of Applied Materials, KIT, Haid-und-Neu-Str. 7, 76131 Karlsruhe, Germany
[b]Sirona Dental Systems GmbH, Fabrikstr. 31, 64625 Bensheim, Germany
[c]Intel Corporation, 5000 West Chandler Blvd, Chandler, AZ 85226, USA
[d]Department of Materials Science and Engineering, CMU, 5000 Forbes Ave, Pittsburgh, PA 15213, USA
[e]School of Materials Engineering, Purdue University, 701 West Stadium Ave, West Lafayette, IN 47907-2045, USA

Abstract—In this study, the equilibrium crystal shape (ECS) of a model system, strontium titanate, is compared with the grain boundary plane distribution (GBPD) as a function of temperature. Strontium titanate has a pronounced surface energy anisotropy and a grain growth anomaly, with the grain growth rate decreasing by orders of magnitude with increasing temperature. The ECS was determined from the shape of small intragranular pores and the GBPD was determined from orientation measurements on surfaces, with the relative areas of grain boundary planes in a polycrystal correlated to the surface energy of both adjacent crystal planes. The grain boundary energy has been previously proposed to be the sum of the surface energy of the adjacent grains less a binding energy that is assumed to be constant. While much experimental evidence exists for this assumption at a fixed temperature, the influence of temperature is not known. While the anisotropy of the ECS was found to decrease with temperature, the anisotropy of the GBPD increased with temperature. These findings indicate that changes in the binding energy with temperature must be considered, as the binding energy links the surface energy to the grain boundary energy. The results are discussed with respect to the grain growth anomaly of strontium titanate, in which the grain growth decreases with increasing temperature.
© 2014 Acta Materialia Inc. Published by Elsevier Ltd. All rights reserved.

Keywords: Equilibrium crystal shape; Grain boundary plane distribution; Surface energy; Strontium titanate; Binding energy

1. Introduction

Grain growth in strontium titanate shows a remarkable anomaly, with the growth rate decreasing over the temperature range of 1300–1390 °C [1–3]. The anomaly was observed using an isotropic grain growth law to determine the growth rate constant,

$$D^2 - D_0^2 = kt = 2\alpha\gamma m \cdot t \tag{1}$$

where D is the grain size, D_0 is the grain size at time $t = 0$, γ is the grain boundary energy, m is the grain boundary mobility, α is a geometric constant close to 1 [4] and $k = 2\alpha\gamma m$ is the grain growth rate constant, combining the grain boundary energy and mobility into a single parameter [3]. In strontium titanate, k does not follow a single Arrhenius equation; instead, it drops significantly between 1300 and 1390 °C, as shown in Fig. 1.

In alumina, adsorption (complexion) transitions of the grain boundaries with dopant composition are known to change the grain boundary mobility and thereby the grain growth rate by similar orders of magnitude [5–7]. However, the situation is different for strontium titanate: no dopants are introduced that might lead to the observed non-Arrhenius behavior of the grain growth rate. The observed behavior may be a result of changes in the grain boundary structure and stoichiometry with temperature, leading to changes in the grain boundary energy and/or mobility. The grain boundary stoichiometry of strontium titanate was observed by transmission electron microscopy [8]; Ti-rich grain boundaries were found to be slower than others. However, no clear correlation to the grain growth anomaly seems to exist.

A change in grain boundary faceting of strontium titanate with temperature was proposed to explain the non-Arrhenius behavior [1]; it is well known that both grain boundary energy [9] and mobility [10,11] are anisotropic. Bäurer et al. suggested a decrease with temperature in the relative grain boundary energy of the low mobility boundaries [1]. This transition would result in an increasing fre-

* Corresponding author. Tel.: +49 721 608 47922; e-mail: wolfgang.
 rheinheimer@kit.edu
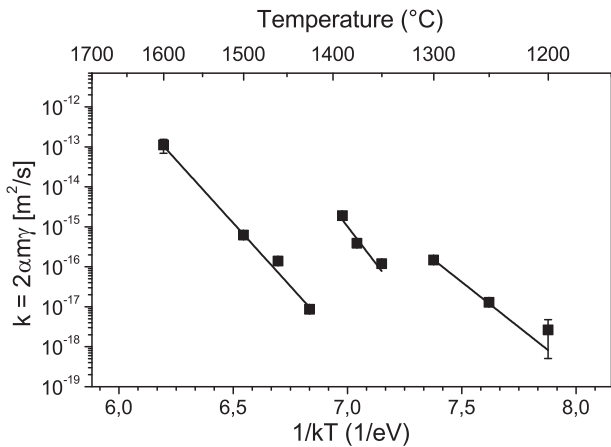
Fig. 1. Plot of the grain growth rate constant $k = 2\alpha\gamma m$ as a function of inverse temperature for strontium titanate in oxygen [3].

quency of low-energy, low-mobility grain boundaries in the microstructure and a reduction in the grain growth constant.

The rationale for this relationship derives from the work of Saylor et al., in which the frequency of specific grain boundary planes in dense polycrystalline $SrTiO_3$ and MgO was related to their surface energy anisotropy [12,13]. The relative areas of grain boundary planes (grain boundary plane distribution, GBPD) are determined by serial sectioning and orientation mapping via scanning electron microscopy (SEM), electron backscatter diffraction (EBSD) [12–15] or a stereological reconstruction of the 3-D microstructure information on a single plane [15–17]. They observed that the frequency of specific grain boundary planes corresponding to low-index surface orientations of one of the two grains increased as the relative surface energy decreased for these two systems, each examined at a single temperature [12,13]. The question for strontium titanate is whether this relationship still holds as the relative surface energies change as a function of temperature. Due to the observed grain growth anomaly with temperature and pronounced surface energy anisotropy, strontium titanate lends itself to a comprehensive study of the influence of surface energy anisotropy (as manifest in the equilibrium crystal shape) on grain growth.

In the work of Saylor et al., the energy of a straight grain boundary has been described by the equation

$$\gamma_{GB} = \gamma_1 + \gamma_2 - B \tag{2}$$

where γ_1 and γ_2 are surface energies and B is the binding energy [6,18,19]. The binding energy relates to the atomic reconstruction of the adjacent crystal lattices when two surfaces are brought together and bonds form across the interface [19]. If the binding energy is assumed to be isotropic, the remaining anisotropy is assumed to be captured in the surface energy terms [6,14,19]. Although the domain of grain boundary types requires a five-dimensional space, Eq. (2) reduces the anisotropy of γ_{GB} to the surface energy anisotropy, which is much easier to access by experiment.

These assumptions may not be valid, however, as the nature of the binding energy must be considered. Its isotropy is an assumption to reduce the parameter space of the grain boundary energy and thereby to simplify experimental considerations of the grain boundary anisotropy. In fact, there is no reason for the binding energy to be

isotropic [14,15,18,20]. A counter example is the case of special grain boundaries with high lattices site coincidence (low Σ) that form a higher number of bonds. Even for a given misorientation, though, the bonding across the interface cannot be constant for all grain boundary plane orientations, and the same is true for different misorientations. Additionally, no information is available on a possible temperature dependence of the binding energy. Comparing the changes in equilibrium shapes, the relative surface energies of specific planes in strontium titanate and the frequency of specific grain boundary planes will allow the range of validity of this equation to be examined.

The equilibrium crystal shape (Wulff shape) reflects the minimization of surface energy of an isolated particle or void [21,22] and directly gives the relative surface energies and anisotropy. However, the observation of the equilibrium crystal shape is difficult due to the kinetics of equilibration. Growing or shrinking particles or voids will generally be bounded by low-mobility planes and not necessarily by the low-energy planes, and will therefore have a kinetic shape [23,24]. Determining the equilibrium shape from a kinetic shape is a central problem in every study of the Wulff shape [25,26]. Different analytical approaches to the equilibration kinetics of particles or pores have been used [25,26], the most important factor for equilibration of an isolated particle or void being its size.

In this study, the Wulff shape of small intragranular pores was used to measure the anisotropy of the surface energy as a function of temperature. In parallel, the GBPD was observed as a function of temperature. The combination of these two methods makes it possible to compare the anisotropy in surface and grain boundary energy and to evaluate their relationship to the observed grain growth anomaly. The resulting dataset can be used to improve sintering and grain growth modeling, as the interface energy is a part of the driving force [4,27] and few anisotropic data are available in the literature. A deeper understanding of the microstructure development in the perovskite model system $SrTiO_3$ is helpful for different applications. For example, most positive temperature coefficient (PTC) devices use perovskite materials [28]; the PTC effect originates from an interaction between a polar crystal structure and the space charge at grain boundaries.

2. Experimental procedure

2.1. Generation of intragranular pores

A sandwich-type specimen was used for the equilibrium shape measurements. Small pores were obtained by joining a strontium titanate single crystal to an $SrTiO_3$ polycrystal. Stoichiometric polycrystalline material was first prepared by a mixed oxide/carbonate route based on high-purity raw materials ($SrCO_3$ and TiO_2, with purities of 99.95 and 99.995%, respectively; Sigma Aldrich Chemie GmbH, Taufkirchen, Germany). Details of the synthesis are published elsewhere [29]. The green bodies were sintered at 1425 °C for 1 h in oxygen to obtain a relative density of more than 99%. Samples were cut into discs and polished (diamond slurry, 0,25 μm), then scratched with a polishing disc (30 μm diamonds) to create pore channels.

The strontium titanate single crystals (impurity content: <10 ppm Si, <2 ppm Ba, <1 ppm Ca; SurfaceNet GmbH, Rheine, Germany) were chemico-mechanically polished

Table 1. Temperatures, atmospheres and dwell times used for the equilibration of pores in strontium titanate.

Temperature (°C)	Atmosphere	Dwell time (h)
1250	Air	740 (not quenched)
1350	O_2	85
1350	N_2–H_2	95
1380	O_2	120
1380	N_2–H_2	100
1460	O_2	54.5
1460	N_2–H_2	46
1600	O_2	53.5
1600	N_2–H_2	25

and placed between two polished and scratched polycrystalline discs. Stacks were joined at 1430 °C for 20 min in air with a load of 1 MPa. During diffusion bonding the pore channels created by the scratches break up into rows of small pores [30]. As the interface between the single crystal and the polycrystal migrates into the polycrystalline matrix, pores become isolated within the single crystal and are used to observe the equilibrium crystal shape.

The sandwich samples were equilibrated at temperatures between 1250 and 1600 °C in oxygen or a mixture of 95% nitrogen and 5% hydrogen ($p(O_2) \approx 8 \times 10^{-8}$ Pa). Details of the heat treatments are shown in Table 1. The dwell times were interrupted for grain growth studies, which will be reported in a follow-up paper. To evaluate the influence of the interrupted anneals, two different samples were compared, one of which was cooled from 1380 °C at 10 K min^{-1} while the other was quenched from 1380 °C at more than 200 K min^{-1}. The pore shapes in both samples were analyzed, and no significant difference was detected. Hence the influence of the interrupted annealing on the equilibrium shape was determined to be insignificant. At all heat treatments above 1250 °C the samples were quenched to room temperature at ~200 K min^{-1}. The experiment at 1250 °C was cooled in air without quenching.

The pore shape was observed by SEM imaging (Leo 1530, Carl Zeiss AG, Oberkochen, Germany). Fig. 2 shows a typical cross-section with the relevant isolated pores at the bottom. The size of all measured pores was 1–2 μm (max. 3 μm at high temperatures). At each temperature at least seven pores (typically 10) were analyzed.

To evaluate the 3-D pore shape, the SEM images were compared to calculated the pore shape using the Wulff construction for a fully faceted pore. The energies of the facets
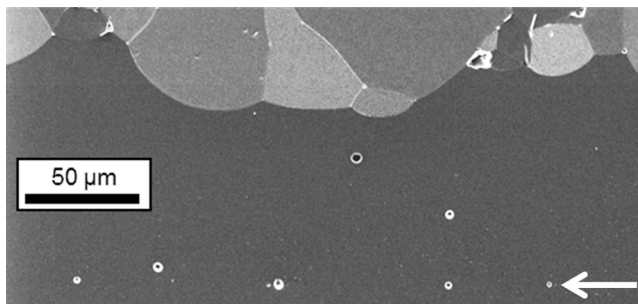
Fig. 2. Typical cross-section observed by SEM of a sample with small pores induced by the bonding of a polycrystal (top) and a single crystal (bottom). The relevant pores can be found on the original interface between the polycrystal and the single crystal (dashed line).

in the Wulff construction were adjusted until the calculated shape fitted the observed shape [31].

2.2. Characterization of the GBPD

The measurement of the GBPD was based on 2-D orientation mapping by SEM and EBSD. However, looking at 2-D microstructures gives only four of the five degrees of freedom of a grain boundary, i.e. the misorientation of both adjacent grains and one of the two angles characterizing the orientation of the grain boundary plane. The second angle of the grain boundary plane, the inclination, was reconstructed using a stereological technique [15,16]. The reconstruction used a discrete binning of 5°. Both planes of the grain boundaries were included; their frequency was counted with respect to the grain boundary plane area [16].

The processing of polycrystalline samples for the GBPD measurements is similar to the polycrystals described above. Three samples annealed at different temperatures were characterized (Table 2). The microstructures grew normally for all temperatures, as shown in Fig. 3. In a previous study on strontium titanate, in which the GBPD was measured after different annealing times at a single temperature, no significant difference in the GBPD was found [17]. Hence no kinetic influence on the GBPD seems to exist.

It was shown previously that similarly processed polycrystalline strontium titanate has no significant misorientation texture [14,32]. All samples were heated in oxygen and subsequently quenched at more than 200 K min^{-1} to prevent any influence of cooling.

3. Results and discussion

3.1. Pore shape and facets

Fig. 4a and b shows a typical pore along with the calculated shape. The main facets of the pores were indexed as {100}, {110} and {111}, based on the cubic symmetry of the perovskite structure. In some cases a facet near {100} was observed, and was indexed as {310} through measurement of its angle to {100} in a cross-section parallel to {100}, as shown in Fig. 4c.

Fig. 5a–d shows the observed pore shape between 1250 and 1600 °C in oxygen, with Fig. 5e–h showing the respective reconstructed shapes. The main facets are {100}, {110} and {111}, which are the most common orientations reported in strontium titanate [9,13,14,33]. At 1460 °C a {310} facet appears in the pores, a facet orientation that has also been observed previously in strontium titanate [9,34,35]. With increasing temperature the pores became more isotropic, i.e. the anisotropy in the surface energy decreased.

Table 2. Heat treatment, mean grain diameter and number of grain boundaries for the observation of the GBPD. All samples were heated in oxygen and subsequently quenched.

Heat treatment	Mean grain diameter	Number of grain boundaries
1300 °C, 10 h	3.47 μm	55,547
1350 °C, 10 h	3.70 μm	46,553
1425 °C, 4 h	4.48 μm	86,783

(a)

(b)

(c)
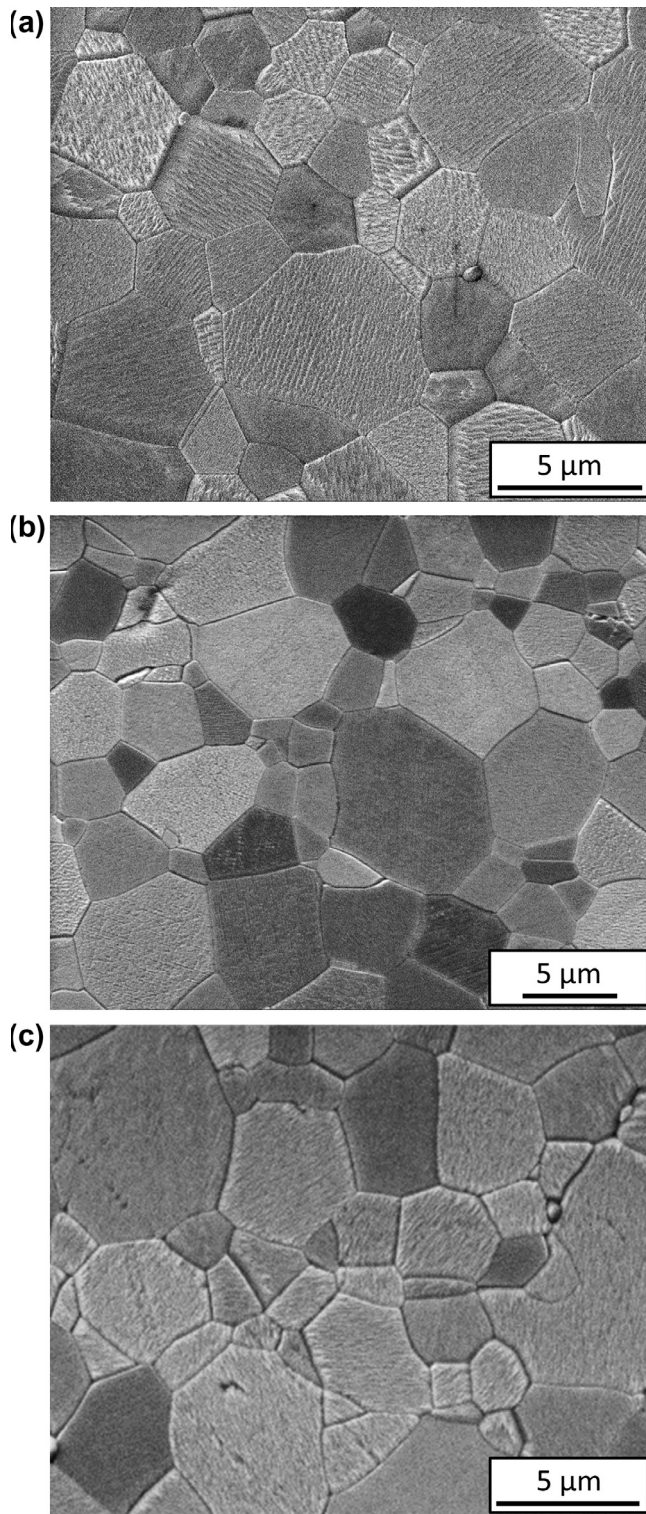
Fig. 3. Microstructures of the samples used for the GBPD heated to (a) 1300 °C, (b) 1350 °C and (c) 1425 °C.

(a)

(b)

(c)

Fig. 4. (a) Shape of a pore observed by SEM. The facets {100}, {110} and {111} are labeled. (b) Reconstructed shape of the pore in (a), with the facets also labeled (c). Measurement of the misorientation of {100} and {310} in a cross-section.

Between some of the facets, microfaceted (corrugated) areas are visible (orange areas in the reconstructed pore shapes in Fig. 5e and f). Their area fraction increases with temperature. The Wulff shape does not contain microfaceted areas [21], but their presence indicates that there must be a constraint on the pore shape, whether kinetic (pinning of the corners or edges) or geometric, due to the presence of saddle-shaped surfaces [36] or quad junctions in the Wulff

shape [37]. The current study only considers the major orientations of strontium titanate. At each temperature the distance from each facet to the center [21] was measured for several pores. Due to the low variance in the data (cf. the error bars in Figs. 7 and 8), no evidence exists for the distance of the main orientations being altered by microfaceting.

The pore shapes between 1350 and 1600 °C in 95% N$_2$– 5% H$_2$ are shown in Fig. 6a–d. The corresponding reconstructed shapes are shown in Fig. 6e and f. The shapes exhibit the same main orientations as those in oxygen, but tend to be more isotropic for the same temperature. Additionally, the pores are more isotropic at higher temperatures, hence the anisotropy decreases. As in oxidizing atmospheres, microfaceted (corrugated) areas are present in the pores.
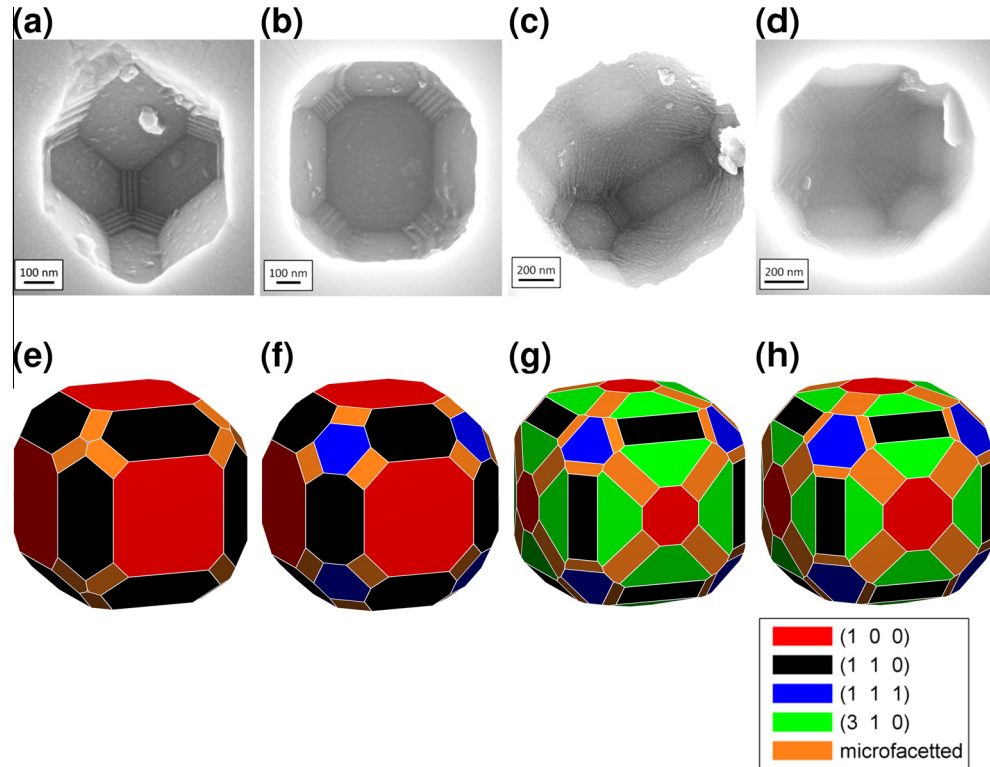
Fig. 5. SEM images of pores annealed in oxygen at (a) 1250 °C, (b) 1380 °C, (c) 1460 °C and (d) 1600 °C. (e–h) Reconstructed pore shapes corresponding to a–d, respectively.

3.2. Relative surface energy

From the Wulff theorem [21], the relative surface energy of a facet in a crystal is proportional to the normal distance from the facet to the center of the shape. Fig. 7 shows the relative surface energy of all low-index orientations observed for temperatures between 1250 and 1600 °C in an oxidizing atmosphere, with all values normalized to {100}, the orientation with the lowest surface energy. The {310} orientation is only visible at 1460 °C or higher. The surface energy anisotropy decreases with increasing temperature.

Sano et al. reported the relative surface energies of {100}, {110} and {111} at 1400 °C in air to be 0.93 ± 0.03, 1.01 ± 0.06 and 1.02 ± 0.01, respectively [9]. These values were renormalized to {100} and are also shown in Fig. 7. The relative surface energy of {110} is in very good agreement with the current study. However, the surface energy of {111} is higher compared to Sano's data. Since Sano's data were obtained by the capillary vector method and in air, this discrepancy is not considered significant.

The relative surface energies of {100}, {110}, {111} and {310} between 1350 and 1600 °C in a reducing atmosphere are shown in Fig. 8. As in an oxidizing atmosphere, the anisotropy decreases with increasing temperature, and {100} exhibits the lowest surface energy. However, {310} is visible at all temperatures. The anisotropy is generally lower than in an oxidizing atmosphere, which is comparable to barium titanate [10,38,39].

A series of studies on barium titanate and strontium titanate related the total vacancy concentration with the faceting behavior of the grain boundaries [10,39,40]. The total vacancy concentration was increased by lowering the oxygen partial pressure or by donor doping (Nd for $BaTiO_3$ and Nb for $SrTiO_3$). The authors reported faceted grain boundaries at low vacancy concentration and unfaceted grain boundaries at high vacancy concentration; this behavior was attributed to a decreasing grain boundary energy anisotropy at high vacancy concentration. The same seems to be true for the surface energy of barium titanate, as the shape of glassy particles embedded in barium titanate is more isotropic in a reducing atmosphere [38]. As shown in Figs. 7 and 8, the surface energy anisotropy of strontium titanate also decreases with decreasing oxygen partial pressure. Accordingly, the decreasing grain boundary energy anisotropy and surface energy anisotropy on decreasing oxygen partial pressure seems to be similar in barium titanate and strontium titanate.

3.3. Distribution of the grain boundary planes

The GBPDs at 1300, 1350 and 1425 °C are shown in Fig. 9. The color represents multiples of random distribution (MRD) and is normalized by grain boundary area. At 1425 °C (Fig. 9c), the GBPD in this study is almost identical to the GBPD at 1650 °C described in the literature [13,14]. All distributions show a similar profile, with a maximum at {100}, a minimum at {111} and a smooth transition in between. However, the width of the distribution between the maximum at {100} and the minimum at {111} increases with increasing temperature, as can be seen from Table 3. Therefore, the anisotropy in the GBPD increases with increasing temperature, with the fraction of grain boundaries parallel to {100} of one of the adjacent grains increasing with temperature.
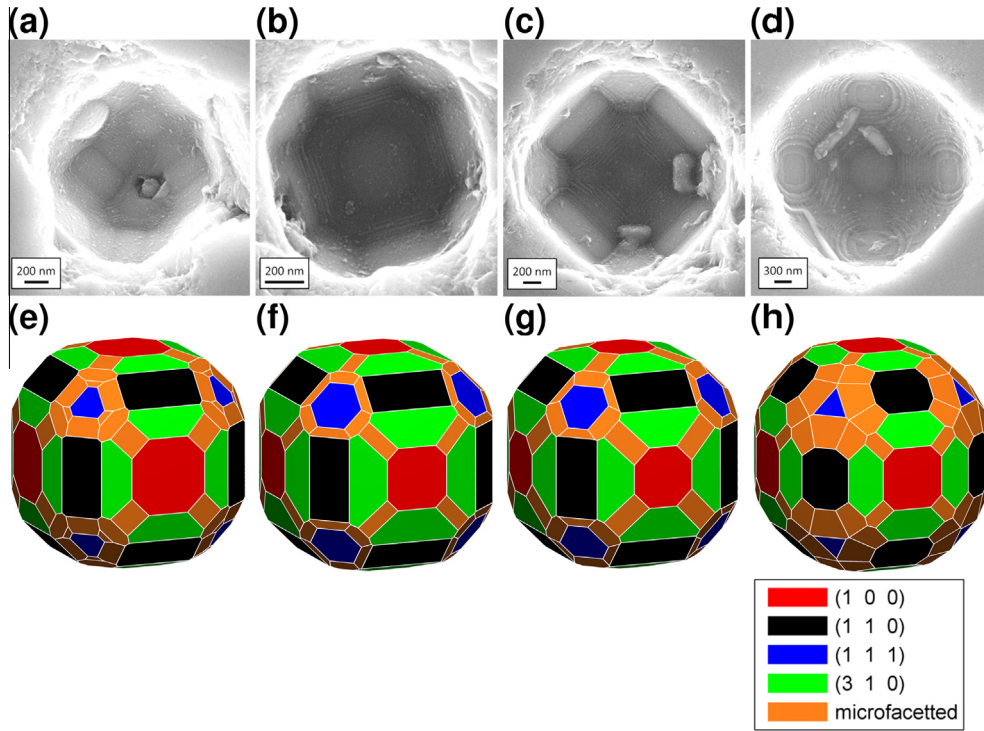
Fig. 6. SEM images of pore annealed in 95% N_2–5% H_2 at (a) 1350 °C(b), 1380 °C, (c) 1460 °C and (d) 1600 °C. (e–h) Reconstructed pore shapes corresponding to a–d, respectively.

These findings are unexpected, if the anisotropy of the grain boundary energy follows the temperature dependence of the surface energy anisotropy alone [19,41,42]. However, studies on the grain boundary faceting in strontium titanate [1,8,32,43,44] and on the temperature dependence of the GBPD in alumina [45,46] and yttria [47] showed similar behavior [1,8,32,43,44]. In strontium titanate at 1300 °C, no grain boundary planes oriented parallel to {100} were observed [1]. At 1425 °C, almost 50% were found to be oriented in {100} with respect to one of the adjacent grains [8]. Shih et al. [43] reported that grain boundaries oriented in {100} are more frequent than expected; concurrently {110} and {111} are slightly less frequent than expected. In summary, the GBPDs in Fig. 9 are consistent with the grain boundary faceting of strontium titanate reported previously. In alumina and yttria, the anisotropy of the GBPD was observed to increase with temperature (as here for strontium titanate) and is correlated to a complexion transition that alters the grain boundary energy distribution [45–47].

3.4. The relationship between the equilibrium crystal shape and the GBPD

It has been shown for several materials that the grain boundary planes in a polycrystal are dominated by the crystallographic planes of the Wulff shape [13], and the frequency of a grain boundary plane is correlated with the inverse of its relative grain boundary energy in several material systems [15,19,20,48]. Hence the GBPDs shown in Fig. 9 indicate an increasing anisotropy in the grain boundary energy with increasing temperature.

Following Eq. (2), the grain boundary energy is composed of the surface energies of both adjacent grains less the binding energy. Usually the latter is assumed to be constant for all grain boundary configurations except special misorientations, providing a high coincidence of adjacent crystal lattices sites [6,14]. In strontium titanate these special orientations were shown in several studies to play no prominent role in the microstructure [14,15,32,43,49,50]. Hence high grain boundary energy corresponds to high surface energy following Eq. (2). In this context, the GBPDs shown in Fig. 9 should be correlated to the surface energy. However, the relative surface energy in Fig. 7 shows a decreasing anisotropy for higher temperatures. Hence a significant difference exists between the anisotropy of the pore shapes and of the anisotropy predicted from the GBPD and Eq. (2).

The origin of the difference is most likely attributable to the temperature dependence of the binding energy, shown schematically in Fig. 10a. The absolute surface energies of the Wulff orientations decrease with temperature. The binding energy decreases with increasing temperature as well; however, the rate is assumed to be lower. It is reasonable that the temperature dependence of the binding energy would be similar to the temperature dependence of the crystal moduli and lower than the dependence of the surface energy due to large number of broken bonds at the surface. According to Eq. (2) the anisotropy, A_{GB}, of the grain boundary energy can be defined as

$$A_{GB} = \frac{\gamma_{GB}^{max}}{\gamma_{GB}^{min}} = \frac{2\gamma_{max} - B}{2\gamma_{min} - B} \qquad (3)$$

where γ_{max} and γ_{min} ($\gamma_{max} > \gamma_{min}$) are the maximum and minimum surface energy, respectively. Equally, the surface energy anisotropy A_{surf} can be defined as

$$A_{surf} = \frac{\gamma_{max}}{\gamma_{min}} \qquad (4)$$
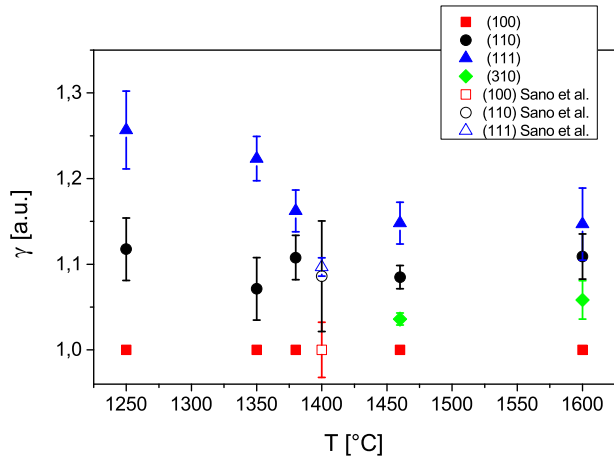
Fig. 7. Relative surface energy of the orientations {100}, {110}, {111} and {310} in oxygen obtained by the inverse Wulff construction (closed symbols). The data of Sano et al. [9] are added (open symbols) for comparison.
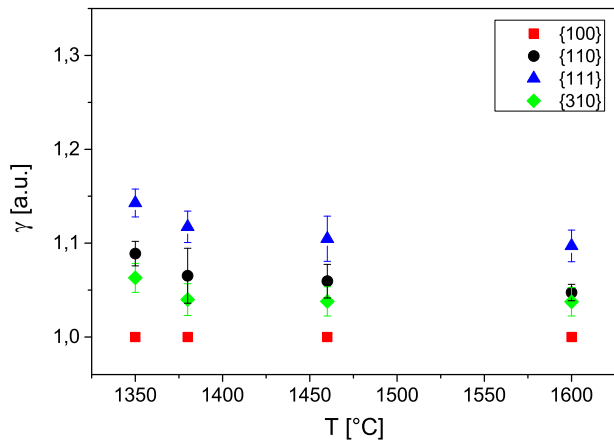
Fig. 8. Relative surface energy of the orientations {100}, {110}, {111} and {310} in 95% N_2–5% H_2 obtained by the inverse Wulff construction.

The binding energy was assumed to decrease more slowly than the surface energy with temperature, which is mathematically equivalent to an increase in B at a fixed A_{surf}. Then A_{GB} increases with B. However, even if A_{surf} decreases (e.g. $\gamma_{max} \rightarrow \gamma_{min}$), an increase in A_{GB} with B is

still possible (e.g. $B \rightarrow 2\gamma_{min}$ results in $A_{GB} \rightarrow \infty$). The sketch in Fig. 10 a gives the temperature-dependent A_{GB} and A_{surf}, as shown in Fig. 10b. According to Fig. 10b, an increase in the grain boundary energy anisotropy with temperature is possible even if the surface energy anisotropy decreases.

The framework sketched in Fig. 10 may explain the difference in the anisotropy of the pores and the GBPD. The pores directly give the relative surface energies and anisotropy. The frequency of grain boundary planes inversely correlates to the grain boundary energy anisotropy [14,20]. The decrease in the surface energy anisotropy (observed by the pore shapes) in conjunction with an increasing grain boundary energy anisotropy (observed by the GBPD) with temperature would result in the observed deviation in the temperature-dependent anisotropy of the pores and the GBPD.

The correlation of the GBPD to the surface energy anisotropy is based on the isotropy of the binding energy in Eq. (2). As already mentioned, this assumption was shown to hold for a given temperature. However, the current study shows that a comparison of the GBPD at different temperatures must account for a change in the binding energy.

3.5. The relationship to anisotropic grain growth in strontium titanate

We believe that the temperature dependence of the anisotropy observed by the pores and the GBPD plays a role in the grain growth anomaly. Between 1300 and 1390 °C, k dropped by orders of magnitude [3]. Around 1390 °C, a drop in the surface energy of {111} in combination with a rise of {110} can be identified (cf. Fig. 7); however, since the variation is not very significant, a drastic change in grain boundary faceting is unlikely to be due to the changes in the relative surface energy. Hence the grain growth anomaly cannot be understood just in terms of the surface energy anisotropy.

However, the grain boundary energy anisotropy seems to be related to the grain growth anomaly. The GBPDs presented in Fig. 9 indicate an increasing frequency of grain boundaries oriented in {100} with increasing temperature. This increase occurs in a similar temperature range as the grain growth anomaly discussed in Section 3.3.

In many grain growth simulations even a small fraction of low-mobility grain boundary planes was shown to
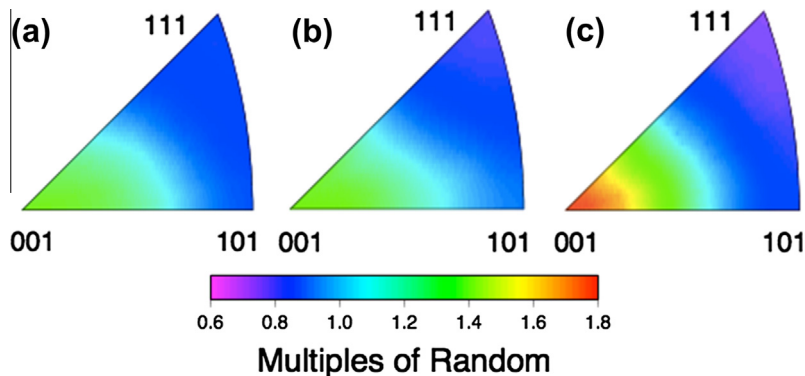
Fig. 9. GBPD of strontium titanate. The samples were heated at (a) 1300 °C, (b) 1350 °C and (c) 1425 °C. The color scale represents MRD and is normalized by the grain boundary area. (For interpretation of the references to colour in this figure legend, the reader is referred to the web version of this article.)

Table 3. Maximum and minimum frequencies of the grain boundary planes for the data shown in Fig. 9.

Temperature (°C)	Min. frequency (MRD)	Max. frequency (MRD)
1300	0.83	1.29
1350	0.80	1.32
1425	0.77	1.70
1650 [13]	0.6	1.75

(a)

(b)
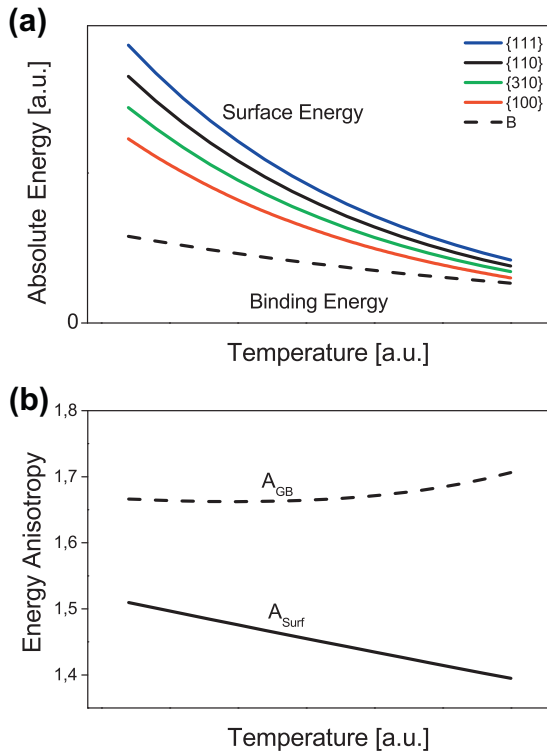
Fig. 10. (a) Sketch of the temperature dependence of the absolute surface energy and the binding energy B of strontium titanate. (b) The resulting surface energy anisotropy A_{Surf} and grain boundary energy anisotropy A_{GB}.

strongly decrease the overall grain growth constant [51,52]. Consequently, in strontium titanate the increasing frequency of grain boundary planes oriented in {100} with temperature may be the basis for the grain growth anomaly. However, few studies of the anisotropy of the grain boundary mobility of $SrTiO_3$ exist. At 1470 °C, experiments on single crystals embedded in a polycrystalline matrix indicate that the mobility of {110} is lower than that of {100} [10,11]. Since no temperature-dependent mobility data are available, the relation between the change in the GBPD and the grain growth rate remains uncertain. In this context, research on the temperature-dependent grain boundary mobility is needed.

4. Summary and conclusion

The relationship between the GBPD and the equilibrium crystal shape of strontium titanate was observed as a function of temperature.

The equilibrium crystal shape was observed by the shape of small intragranular pores. The major facets of the pore shape were found to be {100}, {110} and {111}. The inverse Wulff construction was applied to obtain the relative surface energy of all visible facets. {100} showed the lowest surface energy, followed by {110} and {111}. From 1460 °C in oxygen and for all temperatures in reducing atmospheres, a {310} facet was visible in the equilibrium shapes as well. The anisotropy of the surface energy decreased with increasing temperature and decreasing oxygen partial pressure.

The temperature-dependent GBPD indicated the same low-energy planes found by the pore shapes. However, an increasing anisotropy in the GBPD was found with increasing temperature, pointing towards an increase in the grain boundary energy anisotropy with temperature.

The different behavior of the anisotropy in the pore shapes and the GBPD was explained by a temperature dependence of the binding energy. In this framework, the absolute surface energy is assumed to decrease with temperature at a higher rate than the binding energy. Because the grain boundary energy is the sum of two surface energies less the binding energy, an increase in the anisotropy in the grain boundary energy becomes possible. While previous studies showed that the binding energy of the grain boundary is not significant in the relationship between the GBPD and the surface energy, the current findings indicate that this assumption does not hold with respect to temperature.

The behavior of the anisotropy observed by GBPD was related to the grain growth anomaly of strontium titanate. The GBPD indicates an increasing fraction of grain boundaries oriented in {100}. If these grain boundaries were low-mobility grain boundaries, a decrease in grain growth rate would be plausible. However, further data is needed to reveal the temperature-dependent anisotropy of the grain boundary mobility of strontium titanate.

References

[1] M. Bäurer, H. Störmer, D. Gerthsen, M.J. Hoffmann, Adv. Eng. Mater. 12 (2010) 1230.
[2] L. Amaral, M. Fernandes, M.P. Harmer, A.M.R. Senos, P.M. Vilarinho, J. Phys. Chem. 117 (2013) 24787.
[3] M. Bäurer, D. Weygand, P. Gumbsch, M.J. Hoffmann, Scr. Mater. 61 (2009) 584.
[4] J.E. Burke, D. Turnbull, Prog. Met. Phys. 3 (1952) 220.
[5] S.J. Dillon, M. Tang, W.C. Carter, M.P. Harmer, Acta Mater. 55 (2007) 6208.
[6] M.P. Harmer, J. Am. Ceram. Soc. 93 (2010) 301.
[7] P.R. Cantwell, M. Tang, S.J. Dillon, J. Luo, G.S. Rohrer, M.P. Harmer, Acta Mater. 62 (2014) 1.
[8] M. Bäurer, S.J. Shih, C. Bishop, M.P. Harmer, D. Cockayne, M.J. Hoffmann, Acta Mater. 58 (2010) 290.
[9] T. Sano, D.M. Saylor, G.S. Rohrer, J. Am. Ceram. Soc. 86 (2003) 1933.
[10] S.Y. Chung, D.Y. Yoon, S.J.L. Kang, Acta Mater. 50 (2002) 3361.
[11] S.J.L. Kang, S.Y. Chung, J. Nowotny, Key Eng. Mater. 253 (2003) 63.

[12] D.M. Saylor, A. Morawiec, G.S. Rohrer, Acta Mater. 51 (2003) 3663.
[13] D.M. Saylor, B. El-Dasher, Y. Pang, H.M. Miller, P. Wynblatt, A.D. Rollett, et al., J. Am. Ceram. Soc. 87 (2004) 724.
[14] D.M. Saylor, B. El-Dasher, T. Sano, G.S. Rohrer, J. Am. Ceram. Soc. 87 (2004) 670.
[15] G.S. Rohrer, D.M. Saylor, B. El-Dasher, B.L. Adams, A.D. Rollett, P. Wynblatt, Z. Metall. 95 (2004) 197.
[16] D.M. Saylor, B.S. El-Dasher, B.L. Adams, G.S. Rohrer, Metall. Mater. Trans. A Phys. Metall. Mater. Sci. 35A (2004) 1981.
[17] H.M. Miller, G.S. Rohrer, Applications of Texture Analysis, John Wiley & Sons, New York, 2008, p. 335.
[18] D. Wolf, J. Mater. Res. 5 (1990) 1708.
[19] G.S. Rohrer, J. Mater. Sci. 46 (2011) 5881.
[20] D.M. Saylor, A. Morawiec, G.S. Rohrer, Acta Mater. 51 (2003) 3675.
[21] C. Herring, Phys. Rev. 82 (1951) 87.
[22] G.V. Wulff, Z. Krystallogr. Mineral. 34 (1901) 449.
[23] J.S. Wettlaufer, M. Jackson, M. Elbaum, J. Phys. A Math. Gen. 27 (1994) 5957.
[24] R.F. Sekerka, Cryst. Res. Technol. 40 (2005) 291.
[25] W.C. Carter, A.R. Roosen, J.W. Cahn, J.E. Taylor, Acta Metall. Mater. 43 (1995) 4309.
[26] R. Kern, Morphology of Crystals. Part A: Fundamentals, volume A. Tokyo: Terra Scientific Publications; 1987. p. 77.
[27] R. Coble, J. Appl. Phys. 32 (1961) 787.
[28] Y. Chen, S. Yang, Adv. Appl. Ceram. 110 (2011) 257.
[29] M. Bäurer, H. Kungl, M.J. Hoffmann, J. Am. Ceram. Soc. 92 (2009) 601.
[30] M.K. Santala, A.M. Glaeser, Surf. Sci. 600 (2006) 782.
[31] W. Rheinheimer, Zur Grenzflächenanisotropie von SrTiO₃. (Ph.D. thesis), Karlsruhe Institut für Technologie (KIT), 2013. Schriftenreihe des Instituts für Angewandte Materialien 25; ISBN 978-3-7315-0027-8.
[32] S.J. Shih, K. Dudeck, S.Y. Choi, M. Bäurer , M.J. Hoffmann, D. Cockayne, Journal of Physics: Conference Series 2008; 94.
[33] M. Syha, W. Rheinheimer, M. Bäurer, E.M. Lauridsen, W. Ludwig, D. Weygand, et al., Scr. Mater. 66 (2012) 1.
[34] S.B. Lee, W. Sigle, W. Kurtz, M. Rühle, Acta Mater. 51 (2003) 975.
[35] S.B. Lee, J.H. Lee, Y.H. Cho, D.Y. Kim, W. Sigle, F. Phillipp, et al., Acta Mater. 56 (2008) 4993.
[36] J.E. Taylor, J.W. Cahn, Acta Metall. 34 (1986) 1.
[37] J.E. Blendell, W.C. Carter, C.A. Handwerker, J. Am. Ceram. Soc. 82 (1999) 1889.
[38] Y.H. Heo, S.C. Jeon, J.G. Fisher, S.Y. Choi, K.H. Hur, S.J.L. Kang, J. Eur. Ceram. Soc. 31 (2011) 755.
[39] S.M. An, S.J.L. Kang, Acta Mater. 59 (2011) 1964.
[40] Y.I. Jung, S.Y. Choi, S.J.L. Kang, Acta Mater. 54 (2006) 2849.
[41] M. McLean, H. Mykura, Surf. Sci. 5 (1966) 466.
[42] P. Wynblatt, D. Chatain, Rev. Adv. Mater. Sci. 21 (2009) 44.
[43] S.J. Shih, C. Bishop, D. Cockayne, J Eur Ceram Soc 29 (2009) 3023.
[44] S.J. Shih, S. Lozano-Perez, D.J.H. Cockayne, J Mater Res 25 (2010) 260.
[45] S.A. Bojarski, M. Stuer, Z. Zhao, P. Bowen, G.S. Rohrer, J. Am. Ceram. Soc. 97 (2014) 622.
[46] S.J. Dillon, H. Miller, M.P. Harmer, G.S. Rohrer, Int. J. Mater. Res. 101 (2010) 50.
[47] S.A. Bojarski, S. Ma, W. Lenthe, M.P. Harmer, G.S. Rohrer, Metall. Mater. Trans. A Phys. Metall. Mater. Sci. 43A (2012) 3532.
[48] G.S. Rohrer, Annu. Rev. 35 (2005) 99.
[49] S.J. Shih, M.B. Park, D.J.H. Cockayne, J. Microsc. Oxford 227 (2007) 309.
[50] M.B. Park, S.J. Shih, D.J.H. Cockayne, J. Microsc. Oxford 227 (2007) 292.
[51] M. Bäurer, M. Syha, D. Weygand, Acta Mater 61 (2013) 5664.
[52] E.A. Holm, S.M. Foiles, Science 328 (2010) 1138.